Received: 2 September 2022 | Revised: 1 June 2023 | Accepted: 20 June 2023

DOI: 10.1111/all.15837

Allergy EUROPEAN JOURNAL OF ALLERGY AND CLINICAL IMMUNOLOGY EAACI WILEY

ORIGINAL ARTICLE

Epigenetic responses to rhinovirus exposure in airway epithelial cells are correlated with key transcriptional pathways in chronic rhinosinusitis

Marcus M. Soliai[1,2] | Atsushi Kato[3] | Katherine A. Naughton[2] | James E. Norton[3] | Aiko I. Klinger[3] | Robert C. Kern[4] | Bruce K. Tan[4] | Dan L. Nicolae[5] | Robert P. Schleimer[3] | Carole Ober[1,2] | Jayant M. Pinto[6]

[1]Committee on Genetics, Genomics and Systems Biology, The University of Chicago, Chicago, Illinois, USA

[2]Department of Human Genetics, The University of Chicago, Chicago, Illinois, USA

[3]Department of Medicine, Northwestern University Feinberg School of Medicine, Chicago, Illinois, USA

[4]Department of Otolaryngology-Head and Neck Surgery, Northwestern University Feinberg School of Medicine, Chicago, Illinois, USA

[5]Department of Statistics, The University of Chicago, Chicago, Illinois, USA

[6]Department of Surgery, Section of Otolaryngology-Head and Neck Surgery, The University of Chicago, Chicago, Illinois, USA

Correspondence
Marcus M. Soliai and Carole Ober, Committee on Genetics, Genomics and Systems Biology, the University of Chicago, Chicago, IL, USA.
Email: msoliai@uchicago.edu and c-ober@genetics.uchicago.edu

Jayant M. Pinto, Department of Surgery, Section of Otolaryngology-Head and Neck Surgery, the University of Chicago, Chicago, IL, USA.
Email: jpinto@surgery.bsd.uchicago.edu

Funding information
Ernest S. Bazley Charitable Fund; National Institutes of Health, Grant/Award Number: U19 AI106683, R01 HL129735, R01 AI104733, R01 AI137174,

Abstract

Background: Viruses may drive immune mechanisms responsible for chronic rhinosinusitis with nasal polyposis (CRSwNP), but little is known about the underlying molecular mechanisms.

Objectives: To identify epigenetic and transcriptional responses to a common upper respiratory pathogen, rhinovirus (RV), that are specific to patients with CRSwNP using a primary sinonasal epithelial cell culture model.

Methods: Airway epithelial cells were collected at surgery from patients with CRSwNP (cases) and from controls without sinus disease, cultured, and then exposed to RV or vehicle for 48 h. Differential gene expression and DNA methylation (DNAm) between cases and controls in response to RV were determined using linear mixed models. Weighted gene co-expression analysis (WGCNA) was used to identify (a) co-regulated gene expression and DNAm signatures, and (b) genes, pathways, and regulatory mechanisms specific to CRSwNP.

Results: We identified 5585 differential transcriptional and 261 DNAm responses (FDR <0.10) to RV between CRSwNP cases and controls. These differential responses formed three co-expression/co-methylation modules that were related to CRSwNP and three that were related to RV (Bonferroni corrected $p < .01$). Most (95%) of the differentially methylated CpGs (DMCs) were in modules related to CRSwNP, whereas the differentially expressed genes (DEGs) were more equally distributed between the CRSwNP- and RV-related modules. Genes in the CRSwNP-related modules were enriched in known CRS and/or viral response immune pathways.

Conclusion: RV activates specific epigenetic programs and correlated transcriptional networks in the sinonasal epithelium of individuals with CRSwNP. These novel observations suggest epigenetic signatures specific to patients with CRSwNP modulate response to viral pathogens at the mucosal environmental interface. Determining how

Abbreviations: CRSwNP, chronic rhinosinusitis with nasal polyps; DNAm, DNA methylation; DTC, dynamic tree cut; MD, merged dynamic; RNA-Seq, RNA sequencing; RV, rhinovirus.

R37 HL068546, P01 AI145818 and T32 GM07197

viral response pathways are involved in epithelial inflammation in CRSwNP could lead to therapeutic targets for this burdensome airway disorder.

KEYWORDS
airway epithelium, chronic rhinosinusitis, DNA methylation, gene expression, nasal polyposis

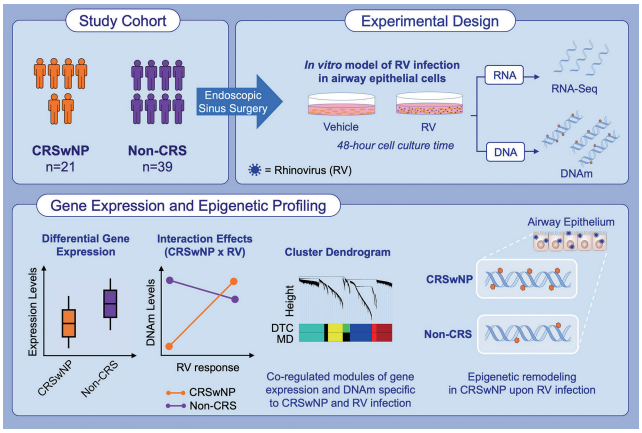

GRAPHICAL ABSTRACT

This study identified differential gene expression and epigenetic profiles of the airway epithelium between chronic rhinosinusitis with nasal polyps (CRSwNP) cases and non-CRS controls in an in vitro cell model. Interaction effects indicated that the epigenetic response to rhinovirus (RV) infection significantly differed between cases and controls. Distinct co-regulated gene expression and DNA methylation modules were specific to CRSwNP and to RV infection. These data suggest that intrinsic epigenetic features in the airway epithelium of CRSwNP influence the response to RV infection and increase susceptibility to CRS.

1 | INTRODUCTION

Chronic rhinosinusitis (CRS) is a common inflammatory disease of the paranasal sinus epithelium.[1] This upper airway disorder is commonly classified clinically into CRS sans nasal polyps (CRSsNP) and CRS with nasal polyps (CRSwNP). These subtypes are associated with different biological profiles[2–4] and environmental risk factors,[5–7] reflecting the heterogeneity of clinical features and (potentially) distinct underlying mechanisms or endotypes.[8,9] A major objective in the field is to identify the genesis of the chronic epithelial inflammation that is the hallmark of this condition. Despite major public health burdens (billions in expenditures on surgery, medication, and testing, major costs for reduced productivity, and significantly impaired quality of life, little is known about underlying molecular mechanisms.

One approach to identifying such pathways has focused on genetic susceptibility, but the few associations reported have not been replicated[10–13] among the relatively few genetic studies to date,[9,10] An alternative approach has been to consider environmental influences, which are plausible drivers of diseases of the upper airway because of its direct interactions with inhaled exposures. Recent evidence supports a such role in CRS.[9,14] Indeed, one major role of the nose is in mucosal immune defense against airborne pathogens. Failure to incorporate a gene–environment interaction perspective may explain (in part) why traditional genetic studies have not been particularly fruitful.

In this study, we examined viral infection as one such environmental trigger that may drive epithelial immune responses in CRS. Several clinical features support this concept. First, patients with CRS are often symptomatic and have exam findings consistent with infection, but bacterial cultures are frequently negative. Second, respiratory viruses in general[15] and rhinovirus (RV) in particular are common in some CRS patients,[16] suggesting a potential role for viral infection in this disease.[16,17] Third, RV induces nasal symptoms (congestion, drainage, etc.) and other clinical features that overlap with CRS.[6,15,18,19] Finally, recent epidemiologic data showed that seasonal patterns of RV infections and CRS exacerbations closely overlap.[20,21] Importantly, direct knowledge of genomic responses to viral infection as a trigger important in CRSwNP remains limited. Curiously, however, a small fraction of adults develop CRS despite billions of RV infections annually in the United States. Taken together, these observations suggest that intrinsic features of the sinus epithelium may drive specific responses to environmental stimuli such as RV infection and cause CRS to develop in susceptible individuals. Therefore, understanding the specific molecular responses to this pathogen could yield insights into disease biology and potentially lead to targeted therapies.

Here, we report the results of a multi-omics study to identify molecular responses to viral infection specific to CRSwNP. To avoid challenges inherent to in vivo studies, we used an upper airway (sinonasal) epithelial cell culture model to identify gene expression and DNAm responses to RV.

2 | METHODS

2.1 | Ethics statement

Sinonasal epithelial cells were collected by brushing from study participants between March 2012 and August 2015 during endoscopic surgeries at Northwestern University Feinberg School of Medicine in Chicago, IL. Informed written consent was obtained from each participant and randomly generated IDs were assigned to all samples to preserve privacy. This study was approved by the institutional review boards of both Northwestern University and the University of Chicago.

2.2 | Cohort description and sample collection

We used a systems biology approach to identify molecular responses to RV that are specific to individuals with CRSwNP. To this end, we designed a cell culture model of RV infection in primary airway epithelial cells (Figure 1).

Sinonasal epithelial cell brushings of the uncinate process were collected from 104 adults during routine endoscopic surgery for CWSwNP (cases) or for other unrelated indications (adenoidectomy, dentigerous cysts, septoplasty, and tonsillectomies) (non-CRS controls). Because the CRSwNP is the most severe CRS phenotype, we focused the design and analysis of this study on a single subtype to reduce the variability in our data.

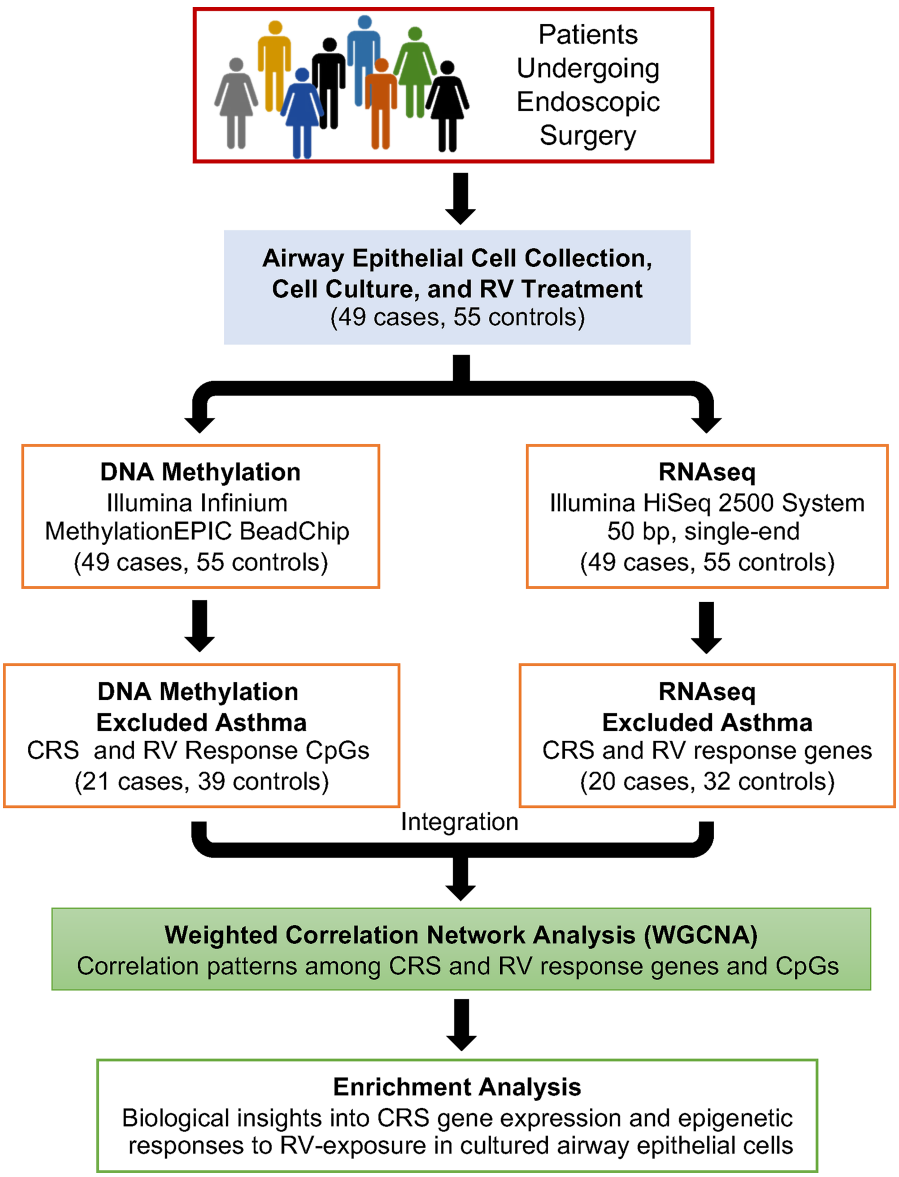

FIGURE 1 Study design and analytical workflow. See methods for additional details.

	Combined	CRSwNP	non-CRS	*p* value
N	60	21	39	–
Sex (% female)	38	14	51	4.45×10^{-6}
Age, median (IQR)	45 (25.25)	54 (14)	38 (22)	3.1×10^{-3}
Race/ethnicity (self-reported)				.60
White	39	15	23	–
Black	13	4	9	–
Hispanic	7	2	5	–
Bi/multiracial	2	–	2	–

TABLE 1 Demographic composition. Ethnicity differences for whites versus other races were tested between CRSwNP and non-CRS participants. Differences in the distribution of sex and ethnicity were evaluated using a chi-squared test, and age was evaluated using a two-sided *t*-test.

The overall cohort included 49 adults with CRSwNP and 55 controls without sinus disease. CRSwNP was diagnosed based on the European Position Paper on Rhinosinusitis and Nasal Polyps (EPOS) criteria.[1] Because asthma is a common co-morbidity with CRS and to avoid identifying pathways that overlap with this lower airway condition, we excluded subjects with a current or previous physician diagnosis of asthma to reduce potential confounding effects. However, after excluding subjects with asthma, only one case and one control had a history of allergic rhinitis and were both included in subsequent analyses.

Based on these criteria, 21 subjects with CRSwNP (cases) and 39 controls (non-CRS) were included in our study. This reduction in sample size had a minimal impact on the statistical power of our analyses for gene expression and DNA methylation, maintaining our capacity to discern significant differences (see Supplementary Methods for details). The demographic characteristics of the study cohort are shown in Table 1.

There were more men than women among the CRSwNP cases, consistent with prior epidemiologic studies.[1] Additionally, the controls were younger, likely reflecting the age distributions of patients requiring surgical intervention for unrelated non-CRS conditions compared to those electing CRS surgery. Age and sex were included as covariates in all subsequent analyses. Ancestry principal components (PCs) were included as covariates to account for genetic ancestry differences between the cases and controls (see below).

2.3 | Airway epithelial cell culture, RV

The airway epithelial cell culture model of RV infection was previously described in detail.[13] Briefly, after isolation at surgery, airway epithelial cells were cultured in bronchial epithelial cell growth medium to near confluence, then cryopreserved at −80°C and stored in liquid nitrogen (range 8 days–3 years). Airway epithelial cells were thawed and assessed for viability using trypan blue staining or lactate dehydrogenase (LDH) assays prior to further processing. Only cells demonstrating a viability exceeding 90% were selected for the study. The viable cells were then cultured to confluence and then treated for 48 h with RV (RV-16; RV) using a MOI of 2 or with a vehicle (bronchial epithelial cell basal medium (BEBM) + gentamicin/amphotericin) alone (2-h treatment followed by a wash in media; 46 h culture time after this). After cell culture, cells were lysed and stored at −80°C until they were batched for DNA and RNA extraction. Cells were tested for pre-existing RV infection by RT-PCR prior to infection with RV-16 and excluded if positive. Samples displaying significant cell death post RV-16 infection were excluded from the study to minimize the risk of skewed results due to the confounding effects of non-viable cells. RV-16 was selected because of the extensive experience with this common serotype in cell culture studies, and because its main receptor, intracellular adhesion molecule 1 (ICAM-1), is present on the sinonasal epithelium.

2.4 | Ancestry principal components

Genotyping was performed using the Illumina Infinium HumanCore Exome+Custom Array. The 676 ancestry informative markers[22] on this array were used to estimate ancestry PCs for each subject, as previously described.[13] The first three ancestry PCs were included in all analyses to correct for population structure and genetic ancestry imbalances between the cases and controls.

2.5 | RNA extraction, sequencing and QC

RNA was extracted from RV- or vehicle-treated cells. cDNA libraries were constructed using the Illumina TruSeq RNA Library Prep Kit v2 and sequenced on the Illumina HiSeq 2500 System (50 bp, single-end) at the University of Chicago Genomics Core. Sample contamination and swaps were not detected using the VerifyBamID software.[23] RNAseq mapping and quality control were applied to the dataset, as described.[13] After quality control, 11,898 autosomal genes in the 20 CRS cases and 32 non-CRS controls remained for downstream analyses.

Principal components analysis (PCA) was used to identify biological and technical sources of variation in the normalized RNAseq dataset. While cryopreservation time (range: 8 days–3 years) was not a significant source of variation, six technical effects contributed to sample variance: technician, days of cell culture, cell lysate

batch, RNA concentration, sequencing pool, and percent of mapped RNAseq reads. Thirteen unknown sources of variation (surrogate variables [SV]) were estimated for the dataset using the SVA R package,[24] after protecting for CRS and RV or vehicle treatment. Corrections for technical effects and SVs in the analyses are described below. These approaches allowed us to remove unwanted variation from the data, enhancing the signal of specific responses of interest.

2.6 | DNA extraction, methylation profiling and QC

Of the 866,836 CpG probes on the EPIC array (Illumina), we removed 74,444 probes that were either located on the X or Y chromosomes, and had detection *p* values greater than 0.01 in more than 10% of samples, or missingness <5%. Quality control and array normalization were applied to each sample, as described.[13] There were 792,392 autosomal CpGs in 21 CRS cases and 39 non-CRS controls which remained after quality control. PCA identified biological and technical sources of variation in the normalized methylation dataset. Variability due to cell harvest date was the only significant technical effect and age, sex, and ancestral PCs 1–3 were significant biological variables. Cryopreservation time was not a significant source of variation. Unknown sources of variation were predicted with the SVA package[24] in R, which estimated 21 SVs after protecting for CRSwNP status and RV or vehicle treatment. These variables were included as covariates in the analysis adjusted for in our analyses, again improving our signal-to-noise ratio.

2.7 | Differential gene expression and DNA methylation analysis

To identify transcribed genes and DNAm sites associated with CRSwNP, RV-response, or both, we used linear mixed effects models to identify differentially expressed genes (DEGs) and differentially methylated CpGs (DMCs), based on M-values, using the limma R package.[25] The models used to identify DNAm and gene expression (Gx) differences in CRS cases and non-CRS controls in vehicle- and RV-treated cells, as well as RV-response genes in CRS and non-CRS samples for each gene or CpG site, followed the general form:

$$Y_{(\text{Gx or DNAm})} \sim \beta_0 + \beta_1 X_{CRS} + \beta_2 X_{Treatment} + \text{covariates}.$$

We used an FDR of 0.10 to control the false positive rate. Biological and technical sources of variation were included as covariates for their respective datasets (described above), as well as age, sex, and ancestry PCs 1–3. To test for interactions between RV-response and CRSwNP on gene expression and on DNAm, we included an interaction term as follows:

$$Y_{(\text{Gx or DNAm})} \sim \beta_0 + \beta_1 X_{Treatment} + \beta_2 X_{CRS} + \beta_3 X_{Treatment \times CRS} + \text{Age} + \text{Sex} + \text{ancPCs} + \text{covariates}.$$

Because of the general sparsity of interaction effects detected in small samples, tests for interaction effects were limited to genes or DNAm sites that were DEGs or DMCs, respectively, in any of the above analyses.

2.8 | Correlation network construction by WGCNA

Gene expression and DNAm correlation networks were constructed using a supervised weighted gene co-expression network analysis (WGCNA),[26] a network analysis method for evaluating the correlation structure of our data and to explore relationships between molecular phenotypes (i.e., gene expression, DNAm). For this analysis, we included the 7474 DEGs and 6254 DMCs identified in the four differential gene expression and DNAm analyses, two exploring differences between cases and controls in RV and vehicle-treated cells ($CRSwNP_{RV}$ vs. $non\text{-}CRSwNP_{RV}$ and $CRSwNP_{vehicle}$ vs. $non\text{-}CRSwNP_{vehicle}$) and two exploring differences in RV response in cases and controls ($CRSwNP_{RV}$ vs $CRSwNP_{vehicle}$ and $non\text{-}CRSwNP_{RV\ vs}$ $non\text{-}CRSwNP_{vehicle}$) at an FDR <0.10 (described above; Figure 2). The covariate-adjusted residuals for the DEGs and DMCs were merged, quantile normalized, and then a weighted adjacency matrix was created for the combined gene expression and DNAm residuals (see Supplementary Methods for details).

2.9 | Protein–protein interaction network construction

The Search Tool for the Retrieval of Interacting Genes database (STRING) is a database of known and predicted protein–protein interactions collected from multiple sources including computational predictions and experimental data. The STRING "Multiple Proteins" search tool (STRING version 11.5; https://string-db.org/) was used to construct protein–protein interaction (PPI) networks based on genes that were included in the WGCNA modules and enriched in any biological process with an adjusted *p* value <.10. The STRING network was then visualized with the Cytoscape software,[27] and highly interconnected regions (clusters) of this network were identified using molecular complex detection (MCOD).[28] Clusters with a MCODE score >6 were considered accurate subnetwork predictions (accuracy >90%). These clusters represent known and/or predicted gene interactions corresponding to genes in the modules identified from WGCNA.

3 | RESULTS

3.1 | Molecular profiles related to CRSwNP

Our first goal was to identify the differences in gene expression ($n = 20$ cases, 32 controls) and DNAm profiles ($n = 21$ cases, 39

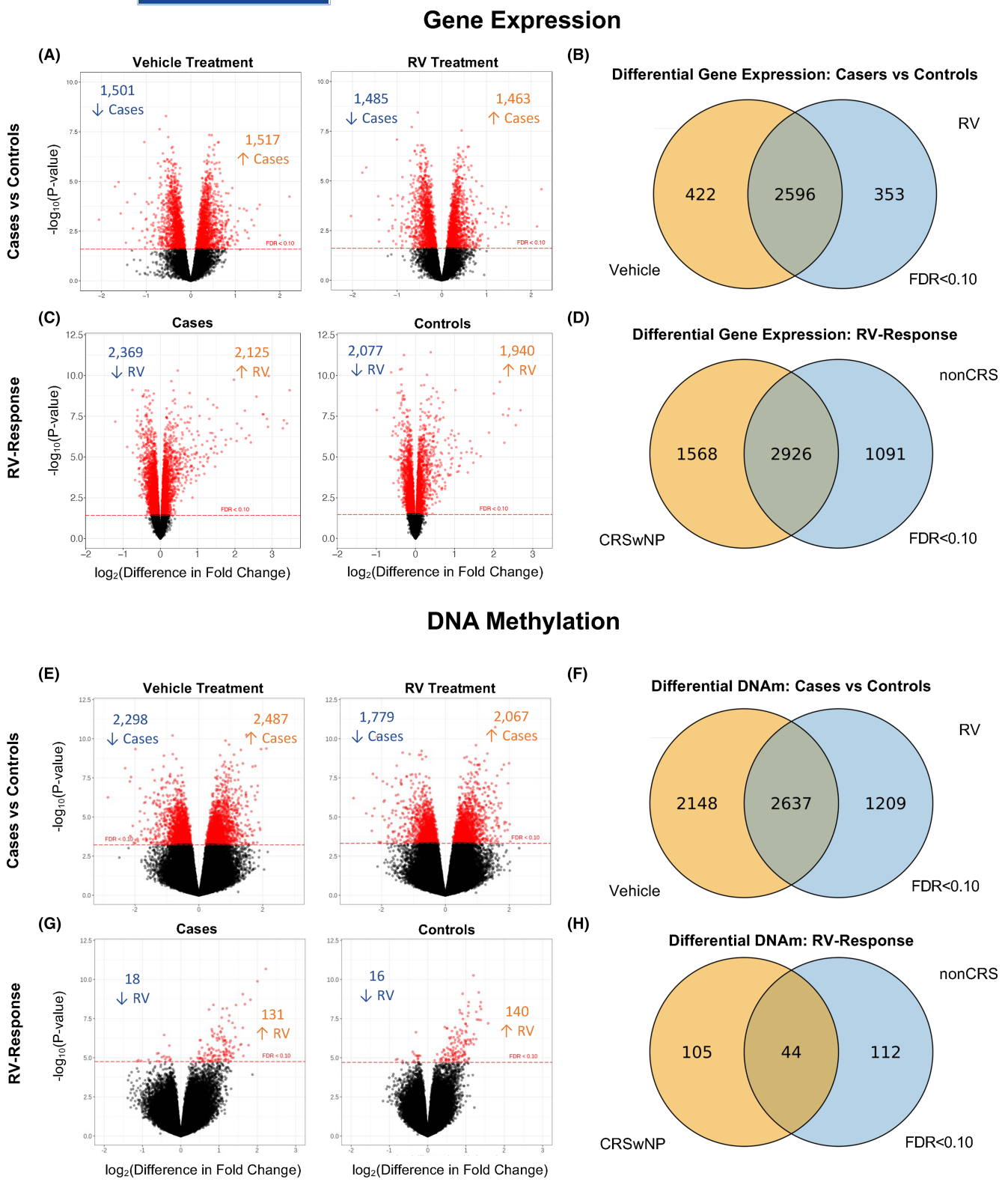

FIGURE 2 Differential gene expression and DNA methylation analysis of cultured airway epithelial cells treated with RV and a vehicle control. (A–D) Results of the differential gene expression analyses. (A) Volcano plots of differentially expressed genes (DEG) between cases and controls from the vehicle-treated cells (left) and the RV-treated cells (right). The red line in each volcano plot indicates a 0.10 FDR threshold. (B) Venn diagram of DEGs from the comparison of cases and controls from the vehicle- and RV-treated cells. (C) Volcano plots of DEGs of RV-response in the cases (left) and controls (right). (D) Venn diagram of RV-responsive genes in the cases and controls. (E–H) Results of the differential DNA methylation analyses. (E) Volcano plots of the differentially methylated CpGs (DMC) between cases and controls in the vehicle-treated (left) and RV-treated (right) cells. (F) Venn diagram of DMCs between cases and controls from the vehicle- and RV-treated cells. (G) Volcano plot of DMCs in response to RV treatment in cells from the cases (left) and controls (right). (H) Venn diagram of RV-responsive CpGs in cases and controls.

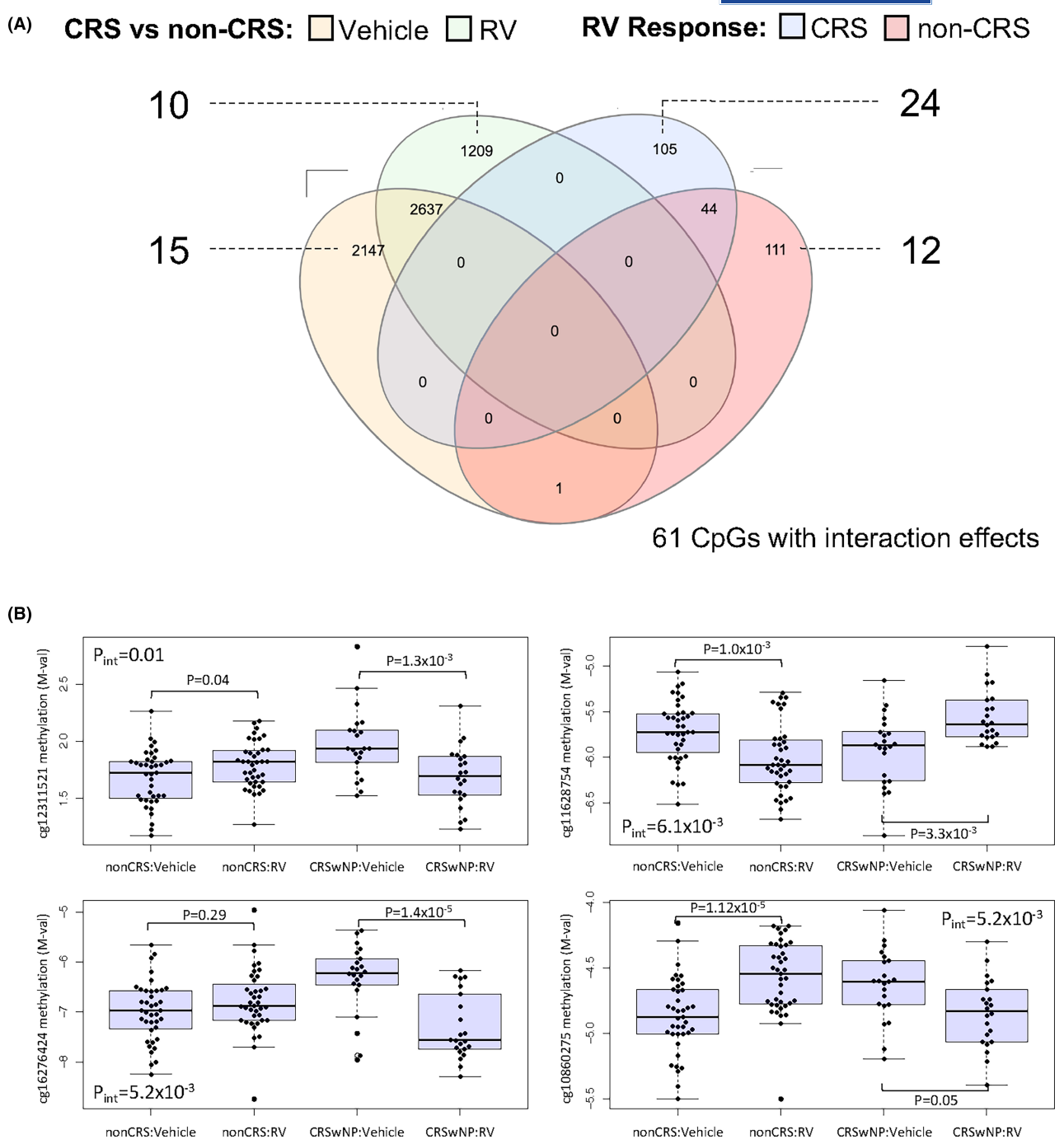

FIGURE 3 DNA methylation (DNAm) sites tested for interaction effects for chronic rhinosinusitis with nasal polyposis (CRSwNP) status and treatment (CRSwNP × treatment). (A) Venn diagram showing the overlap of the 6254 differentially methylated sites at an FDR < 0.10. The numbers on the left and right of the Venn diagram indicate the number of CpGs that were identified to have interaction effects (FDR < 0.10) and the differential analyses from which they were initially identified. (B) Box plots showing examples of DNAm interaction effects for four of the 61 interactive CpGs. The adjusted *p* values for the interaction effects (p_{int}) are shown in each box plot.

controls) between CRSwNP cases and controls and/or between RV- and vehicle-treated samples. To this end, we conducted four analyses each for gene expression and DNAm comparing CRSwNP cases to controls separately in vehicle- and RV-treated cells and comparing RV- to vehicle-treated cells separately in CRSwNP cases and in controls. Overall, 7474 genes were differentially expressed and 6254 CpGs were differentially methylated in at least one of these four analyses. The number of upregulated and downregulated genes and hypomethylated and hypermethylated CpGs in each analysis are shown in Figure 2. CRS × RV interactions were detected for 61 CpGs, reflecting different DNAm responses to RV in cultured airway epithelial cells (Figure 3).

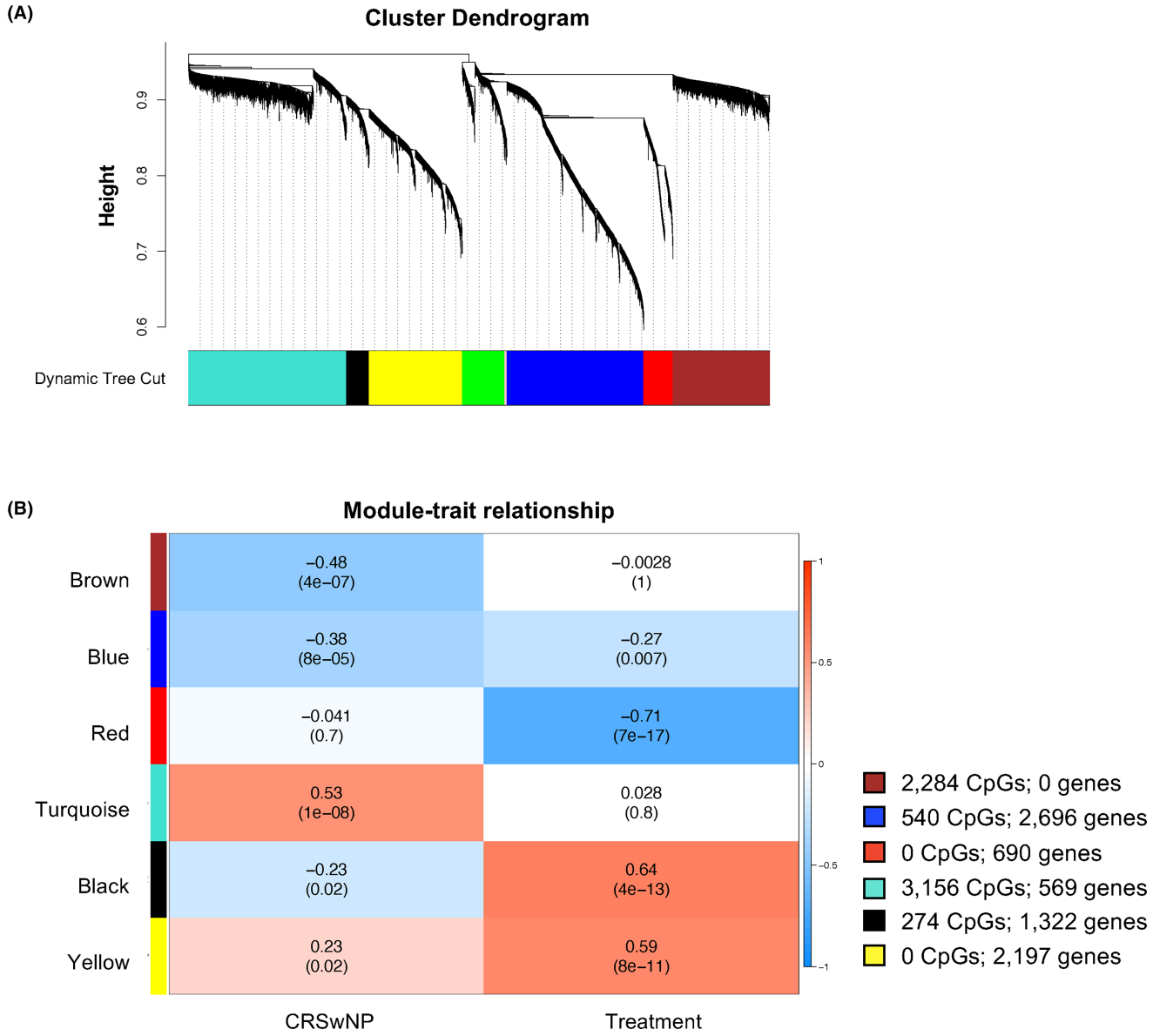

FIGURE 4 Network analysis dendrogram showing co-regulation modules of gene expression and DNA methylation profiles identified by weighted gene co-expression network analysis (WGCNA). (A) Dendrogram showing co-regulated modules of co-expression and DNAm. Colored rows below the dendrogram indicate modules that were identified by WGCNA. The merged modules with highly correlated expression or DNAm profiles are shown on the bottom row. (B) The module–trait relationship. Each row corresponds to a module eigenvector while each column corresponds to either CRS status or treatment. Each cell contains corresponding correlations (top value) and *p* value (bottom value). Cells are colored blue for negative correlations while red cells indicate positive correlations from −1 to 1, respectively. The legend on the right indicates the number of co-regulated genes and DNAm sites in each module.

3.2 | WGCNA identified co-regulated modules of gene expression and DNA methylation specific to CRSwNP

We next used WGCNA,[26] a systems biology tool, to evaluate coordinated transcriptional and epigenetic responses to RV or between cases and controls. For this analysis, we included the 7474 DEGs and 6254 DMCs that were differentially expressed or methylated, respectively in at least one of the four analyses (Figure 2). After merging small, closely related modules (see methods), WGCNA assigned all the DEGs and DMCs to one of six modules of co-regulated gene expression and/or DNAm (Figure 4A). Three modules included both DEGs and DMCs (black, blue, and turquoise), two included only DEGs (red and yellow), and one included only DMCs (brown) (Figure 4B). The correlations (and *p*-values) between the eigenvector of each module with CRSwNP and RV treatment are shown in Figure 4B, identifying three modules correlated with CRSwNP and three modules correlated with RV. Surprisingly, no modules were significantly correlated with both RV infection and CRSwNP after correcting for multiple testing (12 tests, Bonferroni corrected $p < 4.1 \times 10^{-3}$).

The brown, blue, and turquoise modules were significantly correlated with CRSwNP, and the red, black, and yellow modules were

TABLE 2 Module genes enriched in biological pathways. The top five pathways are shown for each module.

	Module (# of pathways p_{adj} <.10)	Term	*p* value	Adjusted *p* value	Odds ratio	Module genes/ pathway genes
RV-Response pathways	Black (4) cell proliferation	Retinoblastoma gene in cancer	4.63×10^{-05}	2.18×10^{-02}	2.96	17/87
		DNA replication	3.18×10^{-04}	7.51×10^{-02}	3.61	10/42
		Breast cancer pathway	5.01×10^{-04}	7.88×10^{-02}	2.16	22/154
		EGF/EGFR signaling pathway	1.00×10^{-03}	9.45×10^{-02}	2.06	22/162
		Signaling pathways in glioblastoma	8.88×10^{-04}	1.05×10^{-01}	2.59	14/82
	Red (67) immune response to microbial infection	The human immune response to tuberculosis	6.35×10^{-19}	3.00×10^{-16}	20.22	16/23
		Type II interferon signaling (IFNG)	3.5×10^{-17}	8.27×10^{-15}	14.14	18/37
		Retinoblastoma gene in cancer	1.24×10^{-14}	1.94×10^{-12}	7.69	23/87
		DNA IR-damage and cellular response via ATR	1.99×10^{-11}	2.34×10^{-09}	6.9	19/80
		Apoptosis	2.34×10^{-08}	2.21×10^{-06}	5.54	16/84
	Yellow (9) lipid and cholesterol biosynthesis	Genes related to primary cilium development	8.29×10^{-13}	3.91×10^{-10}	3.45	39/103
		Cholesterol biosynthesis pathway	9.68×10^{-10}	2.28×10^{-07}	7.3	12/15
		Sterol Regulatory Element-Binding Proteins (SREBP) signaling	5.83×10^{-07}	9.17×10^{-05}	3.04	23/69
		Ciliary landscape	1.57×10^{-04}	1.24×10^{-02}	1.77	42/216
		Lipid metabolism pathway	1.41×10^{-04}	1.33×10^{-02}	3.46	11/29
CRS gene pathways	Blue (10) oxidative phosphorylation	Cytoplasmic ribosomal proteins	1.31×10^{-39}	6.21×10^{-37}	12.93	45/89
		Electron transport chain (OXPHOS system in mitochondria)	1.61×10^{-14}	3.81×10^{-12}	6.46	26/103
		Oxidative phosphorylation	7.66×10^{-10}	1.21×10^{-07}	6.82	16/60
		Mitochondrial complex I assembly model OXPHOS system	1.80×10^{-07}	1.70×10^{-05}	5.94	13/56
		Nonalcoholic fatty liver disease	1.68×10^{-07}	1.98×10^{-05}	3.63	22/155
	Turquoise (1) leptin signaling	Leptin signaling pathway	9.47×10^{-06}	4.47×10^{-03}	5.1	11/76
		IL-5 signaling pathway	8.62×10^{-04}	1.02×10^{-01}	5.28	6/40
		MET in Type 1 papillary renal cell carcinoma	1.36×10^{-03}	1.07×10^{-01}	4.18	7/59
		TNF alpha signaling pathway	1.21×10^{-03}	1.14×10^{-01}	3.44	9/92
		Pathways affected in adenoid cystic carcinoma	4.90×10^{-04}	1.16×10^{-01}	4.33	8/65

significantly correlated with RV, indicating that different molecular changes are related to CRSwNP and RV infection. The three CRSwNP-associated modules were predominantly comprised of DMCs: 95.6% of all DMCs were in the CRSwNP-associated module eigenvectors. The three RV-associated modules included 56.3% of all DEGs, with the remaining 43.6% distributed among two of the CRSwNP-associated modules (blue and turquoise). These data suggested that DNAm patterns may reflect intrinsic properties of airway epithelial cells from CRSwNP patients that modulate the responses of genes to RV infection.

3.3 | Module genes are enriched in CRS and microbial response-associated gene pathways

To infer molecular mechanisms from the genes within the modules, we performed gene enrichment analyses (Enrichr gene enrichment analysis tool)[29] using biological pathways from the WikiPathways database[30] for the five gene-containing modules (Table 2; Supporting Information). The RV-associated modules (red, yellow, black) contained genes enriched in pathways representing particular innate immune responses and molecular signaling pathways involved in response to microbial infection. These pathways have been implicated in the regulation of RV replication in bronchial epithelial cells,[31] and are upregulated by viruses in order to meet the demand for viral structural elements[32] (Table 2). In contrast, the blue and turquoise CRSwNP-associated modules were predominantly enriched in mitochondrial and cytokine signaling molecular pathways respectively. These pathways have been linked to CRS, including genes in the IL-5 and TNF-α signaling pathways[8,9] (*CASP8*, *GRB2*, *MAPK3*, *PTPN11*). Eosinophilic inflammation (where IL-5 plays a critical role)[33] is intimately involved in CRSwNP and TNF-α is involved in initiated relevant immune responses in CRSwNP.[34]

3.4 | DNAm sites with interaction effects are enriched in two modules

To further explore the possibility that some modules may reflect co-regulated pathways of genes and/or CpGs with differential responses to RV between CRSwNP cases and controls, we first assessed the distribution of the 61 DMCs with CRS × RV interaction effects among the four modules containing CpGs (turquoise, black, brown, blue) (Figure 5A). Most of the interactions (86%) included CpGs in two modules: one module was correlated with CRSwNP (turquoise, 32 CpGs) and one module was correlated with RV treatment (black, 21 CpGs). The remaining eight CpGs were in two modules correlated with CRSwNP (brown, 6 CpGs; blue, 2 CpGs). Two of the modules were significantly enriched for DMCs with interaction effects compared to DMCs without interaction effects ($p_{adj} \leq .05$), with a 3.71-fold enrichment in the CRS-correlated brown module ($p = 2.0 \times 10^{-6}$; $p_{adj} = 8.0 \times 10^{-6}$; hypergeometric test) and 7.86-fold enrichment in the RV-associated black module ($p = 3.5 \times 10^{-14}$; $p_{adj} = 1.4 \times 10^{-13}$; Figure 5B). The black module was also enriched for genes involved in proliferative responses, which are important features of both RV response and CRS pathogenesis.

To investigate the regulatory potential of these 61 CpGs, we overlapped their genomic locations with ENCODE31 transcription factor binding sites (TFBS) and tested for enrichments of the CpGs involved in interactions at TFBS relative to CpGs without interaction effects. Indeed, CpGs involved in interactions were enriched 1.28-fold in TFBSs ($p = 5.70 \times 10^{-3}$; hypergeometric test). Overall, 46 of the 61 (75.4%) CpGs overlapped with binding sites for 135 transcription factors, suggesting their potential for influencing the binding of these transcription factors and the expression of their downstream genes. These results demonstrate that DNAm patterns intrinsic to the airway epithelium of CRSwNP patients drive responses to RV by

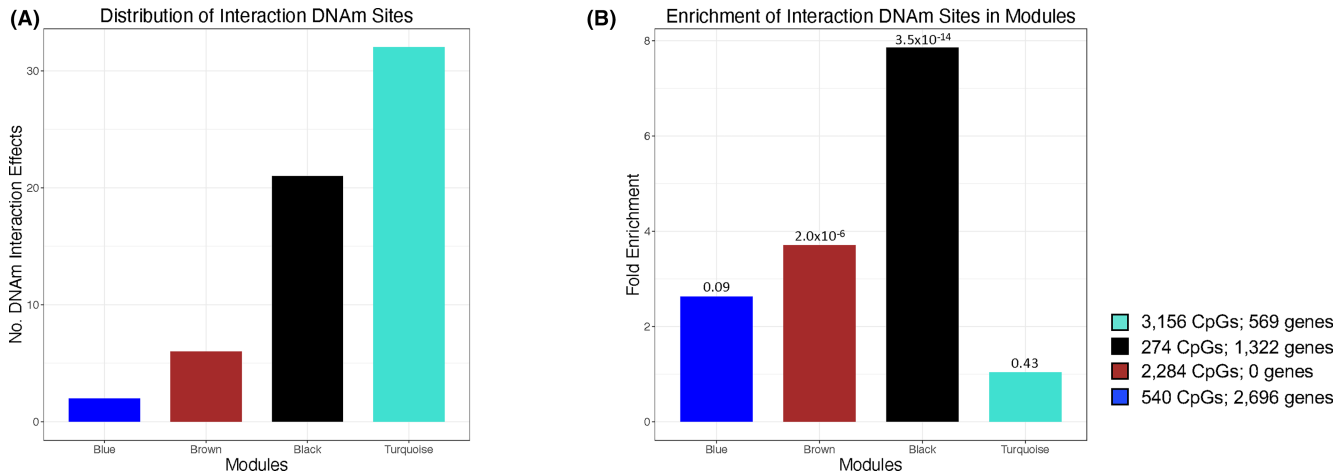

FIGURE 5 Enrichment analysis of DNAm sites with interaction effects in WGCNA modules. (A) Bar plot of the distribution of DNAm sites with interaction effects in modules with co-methylated CpG sites. The x-axis indicates the WGCNA module while the y-axis indicates the number of DNAm sites with interaction effects; the number of DNAm with interaction effects is shown above each bar. (B) Bar plot of enrichments of interaction DNA methylation sites in WGCNA modules. The x-axis indicates the WGCNA module, and y-axis indicates the fold enrichment of interactive DNA methylation sites. Enrichment *p* values for each module are shown above each bar (hypergeometric test).

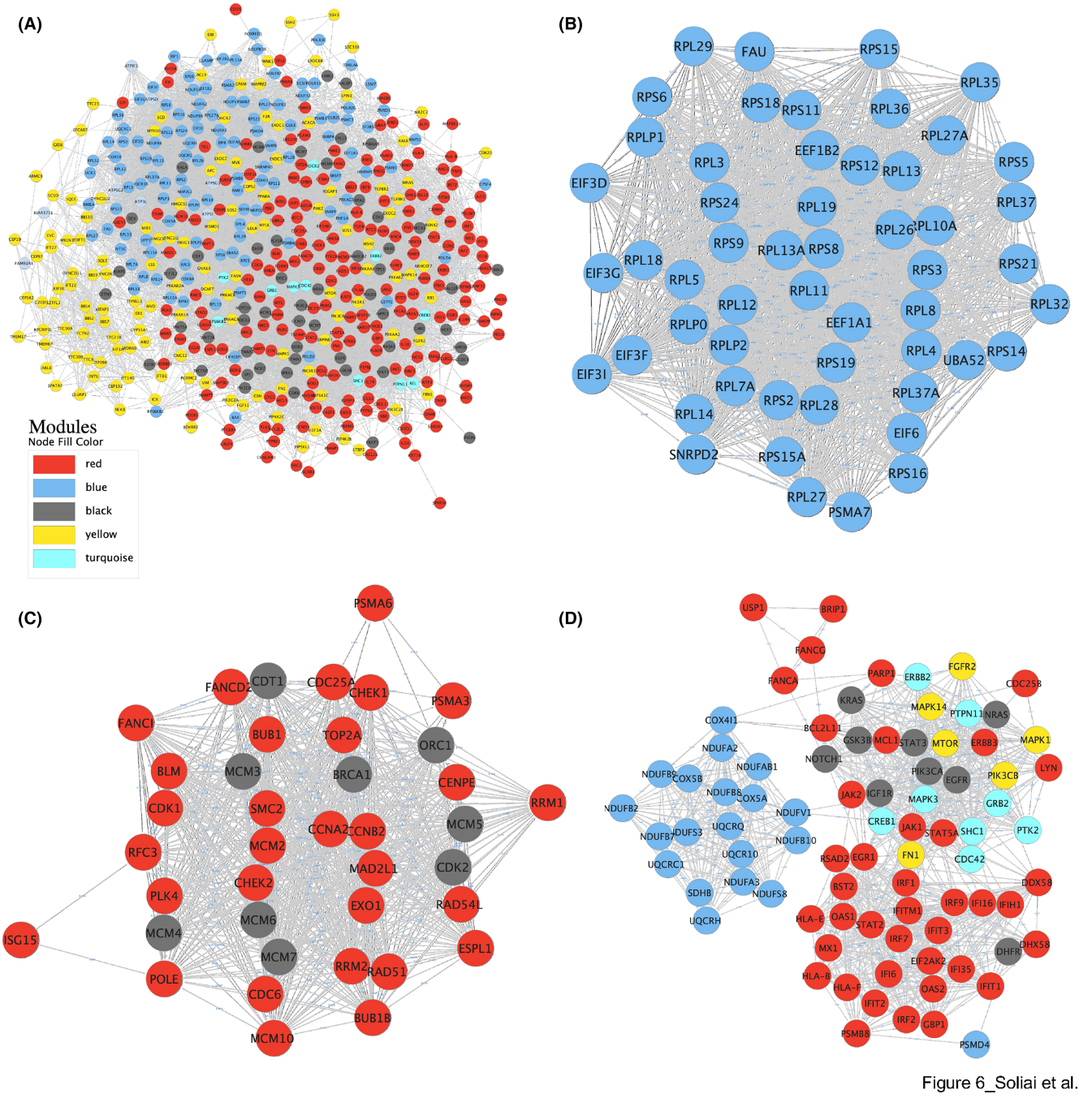

FIGURE 6 PPI network construction and network clusters. (A) PPI network of genes from the five WGCNA modules. Edges show the interaction between two genes and nodes are colored according to the module from which they were assigned. Seven significant clusters identified from the PPI network were determined using MCODE with a score > = 6. The most significant clusters are shown: (B) Cluster 1 with a MCODE score = 52.6. (C) Cluster 2 with a MOCDE score = 32.8. (D) Cluster 3 with a MCODE score = 22.6.

influencing the binding of transcription factors and regulating the expression of coordinated networks of genes.

3.5 | Network analysis shows CRS-associated and RV response gene interactions

The STRING protein–protein interaction (PPI) database was used to construct a gene interaction network of co-expressed genes that were members of the five modules and enriched in biological pathways with a FDR < 0.10. The interaction network was comprised of 508 nodes and 8978 edges (Figure 6A). The molecular complex detection (MCODE) method identified eight clusters of dense protein interactions with scores >6. Although most of these clusters contained module genes in either the CRSwNP-associated (Figure 6B) or the RV-response pathways (Figure 6C), cluster 3 contained module genes in both pathways, potentially linking RV-response (black, red, and yellow modules) to CRSwNP pathogenesis (blue and turquoise

modules) (Figure 6D). The gene membership in Cluster 3 suggests that of the two CRSwNP-associated gene modules, the turquoise module may contain genes that mitigate CRSwNP exacerbation in the presence of RV infection (Figure E4 shows the remaining five modules). The presence of genes identified in Cluster 3 and DMCs with CRS×RV interactions is further support intrinsic DNAm levels driving RV transcriptional responses in the airway epithelium of CRSwNP patients.

4 | DISCUSSION

In this study, we examined the role of a relevant airway pathogen as a trigger of molecular responses in sinonasal epithelium and characterized regulatory gene expression and epigenetic programs that are important in CRSwNP. Using an in vitro model, we showed for the first time that differential epigenetic remodeling occurs in the airway epithelium of CRSwNP patients in response to RV infection, possibly due to intrinsic differences in the epigenetic "wiring" of these critical cells that form the mucosal interface with the environment. Our results further suggested that these CRSwNP-related programs led to dysregulated immune responses to RV, a hallmark of this burdensome disorder. Overall, we identified over 6000 DMCs and 91 biological pathways that may be involved in the CRSwNP, indicating that an altered regulatory response to RV infection results from fundamental differences in the epigenetic landscape in airway epithelial cells and that these differences may drive chronic inflammation in CRSwNP.

Several lines of evidence support these conclusions. First, we observed many DMCs between cases and controls in the vehicle-treated samples (Figure 2E), indicating that epigenetic differences are present after cryopreservation and growth in culture, but in the absence of RV infection, potentially reflecting intrinsic properties of the sinonasal epithelium of individuals with CRSwNP. Second, the vast majority of DMCs were among the three CRSwNP-associated WGCNA modules and distinct from signatures associated with RV treatment. Third, the DMCs with significant CRS×RV interaction effects were enriched for TFBSs, suggesting that variation in these "preprogrammed" DNA methylation profiles may influence the binding of over 100 different transcription factors[35] and downstream expression of their gene targets. Taken together, these findings revealed a central role for epigenetic signatures in the airway epithelium in the pathogenesis of CRSwNP.

Our systems biology approach identified signatures of co-regulated genes that are enriched in pathways previously implicated in CRS or microbial-immune response mechanisms. Of particular note are the two modules (black and brown) that were enriched for DMCs with CRS×RV interaction effects, indicating that the responses to RV significantly differed between the cases and controls. The enrichment for these DMCs at TFBSs suggests that this co-methylation network may direct gene pathways involved in CRSwNP that are triggered by RV. The lack of co-expressed genes in the brown module suggests that the 2284 DMCs in this CRS-associated module may have temporal-specific effects on gene expression outside of the 48-h treatment time point of our cell culture model or during the early stages of disease onset. That is, the DMCs in this module may represent stable, long-term epigenetic states that impact CRSwNP onset (etiology) or progression (pathogenesis) under specific conditions that differ from the context of RV treatment in our model. The finding that the DMCs with interaction effects were also enriched in the RV-correlated black module further supports the notion of an epigenetic regulatory mechanism for genes enriched in cell proliferative pathways in response to RV.

The design of this study provided some advantages for downstream analyses. First, using primary airway epithelial cells from CRSwNP and non-CRS controls to model transcriptional and epigenetic responses to RV infection allowed us to make novel observations of regulatory response mechanisms that are related to CRSwNP. Second, using the same samples for gene expression and DNAm analysis ensured that the results from both analyses were directly comparable and reflected the same biological condition, thereby reducing the variability introduced by inter-individual differences and controlling for potential confounding effects. However, our study had some limitations. First, although we focused on a CRS-relevant tissue cell type (epithelial cells), these studies were in isolation from the many cell types (immune, goblet, others) that may affect mucosal immune response and contribute to CRSwNP. As a result, our model only partially captured physiologic RV-responses and case–control differences that are present in vivo. Second, in vivo studies of molecular responses to RV in CRSwNP face challenges due to (a) variability in exposure to pathogens which can confound or even mask inter-individual responses to RV infection and (b) heterogeneity in clinical disease types (e.g., CRSsNP and CRSwNP, as well as additional subtypes such as allergic fungal rhinosinusitis [AFRS], aspirin-exacerbated respiratory disease [AERD], cystic fibrosis, primary ciliary dyskinesia, and immune deficiencies).[36,37] In vitro cell culture models address these limitations by allowing for controlled environmental exposures in relevant cell types and for precise study designs that minimize confounders to an extent that would be impossible in ex vivo studies. Although the type of cell culture method could affect epigenetic responses (e.g., air-liquid interface cultures),[38] the inherent epigenetic patterns in the mucosal epithelium from CRSwNP should be present in the same cell type in other cell culture methods. Moreover, while the EPIC array is highly accurate and provides valuable insights into the epigenetic patterns associated with RV infection in CRSwNP, analyses are limited to the CpGs and genomic regions that were selected. In particular, arrays have coverage of the human methylome and therefore reduced sensitivity compared to more comprehensive sequencing-based methods. Third, our sample sizes were small, and our power was limited to detect

interaction effects (CRS × RV). It is possible therefore, and even likely, that many more interactions would be detected in larger samples. Finally, this cross-sectional study at a single time point does not allow us to determine whether the epigenetic patterns associated with differential response to RV that is related to CRSwNP preceded and contributed to the onset of disease or was a consequence of the disease state itself. Longitudinal studies that collect ex vivo tissues are needed to address this important question. Similarly, we could not determine whether epigenetic profiles related to RV infection preceded transcriptional changes or if activation of transcription after RV infection led to changes in DNA methylation, as has been shown in innate immune cells responses to bacterial infection.[39]

In summary, we report for the first time that epigenetic programs inherent to the mucosal epithelium from CRSwNP patients may play an important role in pathogen response pathways and lead to chronic inflammation of the upper airway, which has great public health consequences.[40] Focus on the transcriptional networks that are correlated with DNAm and the effects on transcription factor binding in the future could identify novel drug targets or therapeutic modalities specific to CRSwNP.

AUTHOR CONTRIBUTIONS

Marcus M. Soliai prepared the manuscript and performed the computational analyses. Atsushi Kato, Robert P. Schleimer, Dan L. Nicolae, Jayant M. Pinto, and Carole Ober designed the study. Atsushi Kato, James E. Norton, and Aiko I. Klinger performed the cell culture work. Katherine A. Naughton was responsible for sample processing for RNAseq and preparing DNA samples for the Infinium Methylation (EPIC) array and genotyping. Robert C. Kern and Bruce K. Tan performed the surgeries and airways tissue collection. All authors contributed to writing the manuscript. All authors read and approved the final manuscript.

ACKNOWLEDGMENTS

This work was supported by NIH grants U19 AI106683 and R01 HL129735. M.M.S. was supported in part by T32 GM007197.

FUNDING INFORMATION

This work was supported by NIH grants U19 AI106683, R01 HL129735, and by the Ernest S. Bazley Charitable Fund. A.K.'s research was supported in part by NIH R01 AI104733, R01 AI137174, R37 HL068546, U19 AI106683, and P01 AI145818. M.M.S. was supported by NIH T32 GM07197.

CONFLICT OF INTEREST STATEMENT

A.K. received a gift for his research from Lyra Therapeutics; R.P.S. reports consulting fees from Intersect ENT, Merck, GlaxoSmithKline, Sanofi, AstraZeneca/Medimmune, Genentech, Actobio Therapeutics, Lyra Therapeutics, Astellas Pharma, Allakos, and Otsuka. R.P.S. also receives royalties from Siglec-8 and Siglec-8 ligand-related patents licensed by Johns Hopkins to Allakos Inc. B.K.T reports consulting fees from GSK and Regeneron, and speaker fees from Regeneron. R.C.K reports consulting fees from GSK, Lyra Therapeutics, and Regeneron. J.M.P. reports consulting and speaker's bureau fees from Sanofi-Regeneron and Optinose, and participation as a site investigator in clinical trials funded by these same companies and Connect Biopharma. The remaining authors declare that they have no competing interests.

DATA AVAILABILITY STATEMENT

The data that support the findings of this study are openly available in GEO at https://www.ncbi.nlm.nih.gov/geo/query/acc.cgi?acc=GSE172368, reference number GSE172368.

ORCID

Marcus M. Soliai https://orcid.org/0000-0003-3458-0739
Atsushi Kato https://orcid.org/0000-0001-9144-3138
Robert P. Schleimer https://orcid.org/0000-0002-8330-0097

REFERENCES

1. Fokkens WJ, Lund VJ, Hopkins C, et al. European position paper on rhinosinusitis and nasal polyps 2020. *Rhinology*. 2020;58:1-464.
2. Jarvis D, Newson R, Lotvall J, et al. Asthma in adults and its association with chronic rhinosinusitis: the GA2LEN survey in Europe. *Allergy*. 2012;67:91-98.
3. Tan BK, Chandra RK, Pollak J, et al. Incidence and associated premorbid diagnoses of patients with chronic rhinosinusitis. *J Allergy Clin Immunol*. 2013;131:1350-1360.
4. Philpott CM, McKiernan DC. Bronchiectasis and sino-nasal disease: a review. *J Laryngol Otol*. 2008;122:11-15.
5. Gao WX, Ou CQ, Fang SB, et al. Occupational and environmental risk factors for chronic rhinosinusitis in China: a multicentre cross-sectional study. *Respir Res*. 2016;17:54.
6. Jang YJ, Kwon HJ, Park HW, Lee BJ. Detection of rhinovirus in turbinate epithelial cells of chronic sinusitis. *Am J Rhinol*. 2006;20:634-636.
7. Van Zele T, Gevaert P, Watelet JB, et al. Staphylococcus aureus colonization and IgE antibody formation to enterotoxins is increased in nasal polyposis. *J Allergy Clin Immunol*. 2004;114:981-983.
8. Cardell LO, Stjarne P, Jonstam K, Bachert C. Endotypes of chronic rhinosinusitis: impact on management. *J Allergy Clin Immunol*. 2020;145:752-756.
9. Kato A, Peters AT, Stevens WW, Schleimer RP, Tan BK, Kern RC. Endotypes of chronic rhinosinusitis: relationships to disease phenotypes, pathogenesis, clinical findings, and treatment approaches. *Allergy*. 2022;77:812-826.
10. Mitts KB, Chang EH. Genetics of chronic rhinosinusitis. *J Allergy Clin Immunol*. 2020;145:777-779.
11. Kristjansson RP, Benonisdottir S, Davidsson OB, et al. A loss-of-function variant in ALOX15 protects against nasal polyps and chronic rhinosinusitis. *Nat Genet*. 2019;51:267-276.
12. Hsu J, Avila PC, Kern RC, Hayes MG, Schleimer RP, Pinto JM. Genetics of chronic rhinosinusitis: state of the field and directions forward. *J Allergy Clin Immunol*. 2013;131:977-993.e5.
13. Soliai MM, Kato A, Helling BA, et al. Multi-omics colocalization with genome-wide association studies reveals a context-specific genetic mechanism at a childhood onset asthma risk locus. *Genome Med*. 2021;13:157.
14. Park B, London NR Jr, Tharakan A, et al. Particulate matter air pollution exposure disrupts the Nrf2 pathway in sinonasal epithelium via epigenetic alterations in a murine model. *Int Forum Allergy Rhinol*. 2022;12:1424-1427.

15. Cho GS, Moon BJ, Lee BJ, et al. High rates of detection of respiratory viruses in the nasal washes and mucosae of patients with chronic rhinosinusitis. *J Clin Microbiol*. 2013;51:979-984.
16. Basharat U, Aiche MM, Kim MM, Sohal M, Chang EH. Are rhinoviruses implicated in the pathogenesis of sinusitis and chronic rhinosinusitis exacerbations? A comprehensive review. *Int Forum Allergy Rhinol*. 2019;9:1159-1188.
17. Van Crombruggen K, Zhang N, Gevaert P, Tomassen P, Bachert C. Pathogenesis of chronic rhinosinusitis: inflammation. *J Allergy Clin Immunol*. 2011;128:728-732.
18. Lee SB, Yi JS, Lee BJ, et al. Human rhinovirus serotypes in the nasal washes and mucosa of patients with chronic rhinosinusitis. *Int Forum Allergy Rhinol*. 2015;5:197-203.
19. Turner BW, Cail WS, Hendley JO, et al. Physiologic abnormalities in the paranasal sinuses during experimental rhinovirus colds. *J Allergy Clin Immunol*. 1992;90:474-478.
20. Rank MA, Wollan P, Kita H, Yawn BP. Acute exacerbations of chronic rhinosinusitis occur in a distinct seasonal pattern. *J Allergy Clin Immunol*. 2010;126:168-169.
21. Willis AL, Calton JB, Calton J, et al. RV-C infections result in greater clinical symptoms and epithelial responses compared to RV-A infections in patients with CRS. *Allergy*. 2020;75:3264-3267.
22. Tandon A, Patterson N, Reich D. Ancestry informative marker panels for African Americans based on subsets of commercially available SNP arrays. *Genet Epidemiol*. 2011;35:80-83.
23. Jun G, Flickinger M, Hetrick KN, et al. Detecting and estimating contamination of human DNA samples in sequencing and array-based genotype data. *Am J Hum Genet*. 2012;91:839-848.
24. Leek JT, Johnson WE, Parker HS, Jaffe AE, Storey JD. The sva package for removing batch effects and other unwanted variation in high-throughput experiments. *Bioinformatics*. 2012;28:882-883.
25. Ritchie ME, Phipson B, Wu D, et al. Limma powers differential expression analyses for RNA-sequencing and microarray studies. *Nucleic Acids Res*. 2015;43:e47.
26. Langfelder P, Horvath S. WGCNA: an R package for weighted correlation network analysis. *BMC Bioinformatics*. 2008;9:559.
27. Shannon P, Markiel A, Ozier O, et al. Cytoscape: a software environment for integrated models of biomolecular interaction networks. *Genome Res*. 2003;13:2498-2504.
28. Bader GD, Hogue CW. An automated method for finding molecular complexes in large protein interaction networks. *BMC Bioinformatics*. 2003;4:2.
29. Kuleshov MV, Jones MR, Rouillard AD, et al. Enrichr: a comprehensive gene set enrichment analysis web server 2016 update. *Nucleic Acids Res*. 2016;44:W90-W97.
30. Slenter DN, Kutmon M, Hanspers K, et al. WikiPathways: a multifaceted pathway database bridging metabolomics to other omics research. *Nucleic Acids Res*. 2018;46:D661-D667.
31. McCrae C, Dzgoev A, Stahlman M, et al. Lanosterol synthase regulates human rhinovirus replication in human bronchial epithelial cells. *Am J Respir Cell Mol Biol*. 2018;59:713-722.
32. Heaton NS, Randall G. Multifaceted roles for lipids in viral infection. *Trends Microbiol*. 2011;19:368-375.
33. Gevaert P, Han JK, Smith SG, et al. The roles of eosinophils and interleukin-5 in the pathophysiology of chronic rhinosinusitis with nasal polyps. *Int Forum Allergy Rhinol*. 2022;12:1413-1423.
34. Kato A. Group 2 innate lymphoid cells in airway diseases. *Chest*. 2019;156:141-149.
35. Yin Y, Morgunova E, Jolma A, et al. Impact of cytosine methylation on DNA binding specificities of human transcription factors. *Science*. 2017;356.
36. Kato A, Peters AT, Stevens WW, Schleimer RP, Tan BK, Kern RC. Endotypes of chronic rhinosinusitis: relationships to disease phenotypes, pathogenesis, clinical findings, and treatment approaches. *Allergy*. 2022;77:812-826.
37. Tomassen P, Vandeplas G, Van Zele T, et al. Inflammatory endotypes of chronic rhinosinusitis based on cluster analysis of biomarkers. *J Allergy Clin Immunol*. 2016;137:1449-1456.
38. Bukowy-Bieryllo Z, Daca-Roszak P, Jurczak J, et al. In vitro differentiation of ciliated cells in ALI-cultured human airway epithelium - the framework for functional studies on airway differentiation in ciliopathies. *Eur J Cell Biol*. 2022;101:151189.
39. Pacis A, Mailhot-Leonard F, Tailleux L, et al. Gene activation precedes DNA demethylation in response to infection in human dendritic cells. *Proc Natl Acad Sci U S A*. 2019;116:6938-6943.
40. Rudmik L. Chronic rhinosinusitis: an under-researched epidemic. *J Otolaryngol Head Neck Surg*. 2015;44:11.

SUPPORTING INFORMATION

Additional supporting information can be found online in the Supporting Information section at the end of this article.

How to cite this article: Soliai MM, Kato A, Naughton KA, et al. Epigenetic responses to rhinovirus exposure in airway epithelial cells are correlated with key transcriptional pathways in chronic rhinosinusitis. *Allergy*. 2023;00:1-14. doi:10.1111/all.15837